EFFICIENCY AND MASS LOADING CHARACTERISTICS OF A TYPICAL HEPA FILTER MEDIA MATERIAL

V.J. Novick, P.J. Higgins, B. Dierkschiede,
C. Abrahamson and W.B. Richardson
Engineering Physics Division
Argonne National Laboratory
Argonne, Illinois

and

P.R. Monson and P.G. Ellison
Westinghouse Savannah River Company
Aiken, South Carolina

DP-MS--89-1292
DE90 017796

Abstract

The particle removal efficiency of the HEPA filter material used at the Savannah River Site was measured as a function of monodisperse particle diameter and two gas filtration velocities. The results indicate that the material meets or exceeds the minimum specified efficiency of 99.97% for all particle diameters at both normal and minimum operating flow conditions encountered at the Savannah River site.

The pressure drop across the HEPA filter material used at the Savannah River site was measured as a function of particle mass loading for various aerosol size distributions. The pressure drop was found to increase linearly with the particle mass loaded onto the filters, as long as the particles were completely dry. The slope of the curve was found to be dependent on the particle diameter and velocity of the aerosol. The linear behavior between the initial pressure drop (clean filter) and the final pressure drop (loaded filter) implies that the filtration mechanism is dominated by the particle cake that rapidly forms on the front surface of the HEPA filter. This behavior is consistent with the high filtration efficiency of the material.

Introduction

An Airborne Activity Confinement System (AACS) is used in each of the reactors at the Savannah River site to provide for the capture and confinement of accidentally released radioisotopes. Figure 1 presents a schematic description of the AACS.[1] The purpose of the moisture separator (first filter) is to remove the water droplets and any other large aerosol particles before they can be deposited in the High Efficiency Particulate Air (HEPA) filter. The HEPA filter is designed to remove all particles from the gas stream with efficiencies of at least 99.97%.[2] The final component of the filter compartment is a carbon bed. The purpose of the carbon bed is to remove more than 99.9% of the elemental iodine vapors from the exhaust gas.[3]

The purpose of this research was to characterize the HEPA filter media material. This work consisted of three major tasks. The first task was to determine the filtration efficiency spectrum for solid particles as a function of particle diameter. Second, the pressure drop characteristics of the HEPA filter material were measured as a function of the aerosol mass loading. Particle size effects were studied by using different particle size filtration efficiency spectrum for solid particles as a function of particle diameter. The third task was to provide a theoretical foundation that will allow the experiment results from the mass loading tests to be generalized. These tests were conducted at the Argonne National Laboratory between September 1988 and February 1990, under the sponsorship of the Westinghouse Savannah River Company. An experimental apparatus was set up based on filter characterization work discussed in the literature.[5,6] Sodium chloride was chosen as the challenge aerosol based on a number of considerations. Sodium chloride is highly soluble in water, it is non-toxic, and it allows a precise means of analysis by conductivity. Sodium chloride particles produced by atomization are non-spherically shaped. In comparison to spherical particles, they may simulate more closely the shape of particles likely to be produced in the Savannah River Reactor. The filter media was chosen to be identical with the SRP filter material. However, the filter size was chosen to be 47 mm in diameter in order to facilitate laboratory handling and analysis and to minimize the total mass of particles that are needed to be aerosolized. To account for the difference in filtration area, the gas flow rate was scaled such that the velocity through the filter medium was the same for both plant filters and laboratory filters. The gas viscosity is expected to be similar to that encountered at SRP by using air at 25°C. The particle size is an experimental variable since there is uncertainty in the particle size distribution that may be released into the AACS.

Experimental Setup for Efficiency Tests

Figure 2 illustrates the experimental apparatus used for the efficiency tests. The experimental setup can be broken down into two main systems, aerosol generation and aerosol sampling. The aerosol generation system consists of an aerosol nebulizer, a dryer to dry the wet aerosol and a neutralizer to reduce the electrical charge on the aerosol to a Boltzmann equilibrium. The aerosol sampling system consists of a mixing chamber and the aerosol sampling devices.

Typically, filter efficiency spectra are obtained using monodisperse challenge aerosols. In addition, the characterization of the filter efficiency using monodisperse particles would be more useful for later code input for calculating probable scenario dependent releases. A proven method of generating monodisperse aerosols is to use an electrostatic classifier.[7,8] The classifier used in this work is the Model 3071, manufactured by TSI Inc. of St. Paul, Minnesota, capable of producing monodisperse particles ranging from 0.01 μm to 1 μm in diameter.

Data was acquired during the efficiency test, by simultaneously using condensation nucleus counters (CNC's) to measure the filtered and unfiltered particle concentrations from the sampling chamber. The CNC used to measure the unfiltered particle concentration (TSI Model 3020) has an internal mass flow controller, factory set to sample the aerosol at a rate of 0.30 liters/min. The instrument has two particle counting modes, providing a dynamic measurement range of 10^{-2} to 10^{7}

particles/cm^3. The CNC used to measure the filtered particle concentration (TSI Model 3760) operates in only the single-particle mode. Aerosol flow through this CNC is controlled by a critical orifice and an external vacuum pump, providing a constant gas flow rate of 1.415 liters/min. The range of particle concentrations measurable by the Model 3760 extends from 10^{-3} to 10^3 particles/cm^3. For particle concentrations below 10^3 particles/cm^3, the two CNC's simultaneously measured the same aerosol concentration to within 15%.

Efficiency Test Results

Flowrates and voltages on the Electrostatic Classifier were adjusted to provide at least eight different monodisperse particle diameters, ranging from 0.05 μm to 0.5 μm, as challenge aerosol for the filters. The penetration of particles through the filter was measured for each minute by dividing the downstream particle concentration by the upstream particle concentration. The removal efficiency for a given particle size was found by averaging the penetration values over at least 15 minutes and subtracting the average penetration from one. The penetration as a function of time over the 15 minute measurement was observed to be fairly constant, decreasing by only 10% to 20%. This slow decrease in penetration is typically observed as the particle cake forms on the filter's surface.

The filtration efficiency was measured at two different gas velocities. The velocity of 2.98 cm/s through the filter media is typical of normal operating flow rates of the ACCS. The velocity of 0.89 cm/s was tested in order to determine the efficiency for the minimum operating flow rate conditions of the ACCS.

Figures 3a and 3b show the average number penetration as a function of particle size for the two filtration velocities. Figure 3a shows that for a filtration velocity of 0.89 cm/s the maximum penetration occurs near 0.3 μm. This maximum penetration corresponds to a minimum filtration efficiency of 99.99886%. As expected from filtration theory, the efficiency is seen to increase for both larger and smaller particle sizes. This is because the mechanism of filtration for smaller particles is diffusion, which varies inversely with particle size. For particles larger than that producing minimum efficiency, impaction and interception with the fibers increase directly as function of particle size.

For the higher filtration velocity of 2.98 cm/s, the overall penetration increased approximately by a factor of ten and shifted toward smaller particle diameters. In this case, the minimum penetration occurred at approximately 0.15μm, corresponding to a filtration efficiency of 99.9727%. Two additional points are included on this graph. When the efficiency for 0.12 μm particles was first measured, it was noticed that this point did not fall on a smooth curve joining the other points. The efficiency measurement was repeated for this particle size and this time the point did fall very close to the curve defined by the other data points. To investigate repeatability, another test was rerun at 0.199 μm. This time the second measurement was consistent with the first and with the majority of the other data points. Since no procedural error was evident, the error in the first measurement at 0.12 μm was attributed to filter variation. Out of 10 total filters tested at 2.98 cm/s, only this one produced results inconsistent with the others. No inconsistencies were observed at 0.89 cm/s.

Due to the high collection efficiency of the filter material, it is postulated that there will be a rapid formation of a particle cake on the surface of the filter. Therefore, it is expected that the pressure drop behavior of this filter material as it is loaded with a mass of particles, will follow that predicted by particle cake theory.

Theory

A general model describing the increase in pressure drop as a function of mass loading can be found in a variety of sources[9,10]. For high levels of particle mass loadings on filters, it is generally accepted that the total pressure drop across the filter can be written as the sum of the pressure drop across the clean filter plus the pressure drop across the filter cake due to particle loading.

$$\Delta P = \Delta P_o + \Delta P_p \qquad (1)$$

For the range of pressure drops under considerations in these tests, the gas flow through the filter is laminar, allowing equation (1) to be rewritten in terms of the gas velocity.

$$\Delta P = K_1 V + K_2 V M/A \qquad (2)$$

where

V = gas velocity through the media

M/A = particle mass loading per unit area.

The constant K_1 depends on the filter structural properties such as the porosity and thickness of the filter. K_2 is a constant for a given set of particle and cake parameters such as the particle size and cake porosity. This simple model assumes that the particles are solid. Liquid droplets are more difficult to model due to factors such as the wetability of the filter media and the surface tension and viscosity of the liquid. Obviously there is no cake formation with liquid droplets.

The value of K_1 for the filter material tested in this work can be found by measuring the clean filter pressure drop as a function of gas velocity. Figure 4 plots the data and fits a straight line through the data for velocities up to 5 cm/s. The slope of this line is K_1. The value of K_1 is given as 7.97×10^2 g/cm^2 s. The value of K_2 can be determined both theoretically and experimentally. The theoretical analysis first assumes that the layer of particles forming the cake is comprised of isolated spheres far enough apart so the flow around one sphere does not interfere with the flow around a neighboring sphere (i.e., the porosity of the cake, ε, approaches one) and that the Reynold's number, is less than one, then Stoke's Law can be applied to determine K_2.

$$K_{2Stokes} = (18\,\mu)/(CD^2\,\rho_p) \qquad (3)$$

where μ = gas viscosity

ρ_p = particle density

D = particle diameter

C is the Cunningham slip correction factor given as:

$$C = 1 + \lambda/D \; [2.514 + 0.80 \exp(-0.55 \; D/\lambda)] \qquad (4)$$

where λ is the mean free path of the gas. For air molecules at standard conditions the mean free path, λ , is 0.066 μm.

In real situations the spheres touch causing the flow around each sphere to be affected by its neighboring spheres, hence the porosity no longer approaches 1. In order to account for the effect that porosity has on pressure difference, a resistance factor, R, is defined which allows for a real solution of K_2:

$$K_2 = RK_{2Stokes} \qquad (5)$$

At least two different researchers have developed methods of defining resistance factor R[11]. The work of Kozeny and Carman led to a semi-empirical equation that determines the resistance factor to be:

$$R = 2 K_{ck} (1 - \varepsilon)/\varepsilon^3 \qquad (6)$$

where the empirical constant K_{ck} is equal to 4.8 for spheres and 5.0 for irregular shapes. Leith and Allen[10] state that Equation (6) should not be used if e > 0.7.

Alternatively, Rudnick and First[12] developed an equation for R derived from theory and thus does not have an empirical constant as in Equation (6). This equation is given as:

$$R = [3 + 2(1 - \varepsilon)^{5/3}] \; / \; [3 - 4.5 \; (1 - \varepsilon)^{1/3} + 4.5 \; (1 - \varepsilon)^{5/3} - 3(1 - \varepsilon)^2] \qquad (7)$$

Both methods of determining R require a knowledge of the porosity of the particle cake. However, the porosity can only be determined with experimental measurements of the thickness of the deposited cake and the total mass of particles in the cake. R can also be calculated directly from the experimental data without a thickness measurement by combining Equations (1),(2),(3) and (5) to give:

$$R = AC\rho_p D^2 (\Delta P - \Delta P_o)/18 \; \mu VM \qquad (8)$$

Both theoretical and experimental values for the resistance factor R will be discussed in the section describing the results of the filter mass loading tests.

Experimental Setup for the Mass Loading Tests

The sampling chamber allowed for three 47mm filters, a cascade impactor and a Tapered-Element Oscillating Microbalance (TEOM) to simultaneously sample the aerosol stream. Simultaneous measurements of the aerosol particle mass collected by each port, as determined by the average between a gravimetric analysis and conductivity analysis, indicate that the maximum difference between any two ports is 1.1% while the average difference is 0.5%.

To investigate the role particle diameter plays in the mass loading vs. pressure drop on the HEPA filters, a series of tests were designed to load the filters to given values of pressure difference with particle size distributions of different mass median diameters. The different particle size distributions were obtained by using two different nebulizers, changing the solution concentration of NaCl solute and varying the gas velocity through the nebulizer. The polydisperse aerosols used in the mass loading tests were sized before and after each test with a seven-stage inertial cascade impactor.

The basic concept of the experiment remained the same as in the efficiency work. Clean, dry air was supplied to an aerosol nebulizer producing a distribution of droplets. The droplets were then dried and neutralized and the solid aerosol particles were collected for analysis. There were a number of improvements in the experimental setup relative to the efficiency apparatus. A schematic diagram of the equipment used for these tests is given in Figure 5. Connecting transport tubing was shortened and as many components as possible were mounted vertically to minimize particle losses due to settling. An impinger was added after the Retec nebulizers to remove large droplets that were the major factor in forming occasional plugs in the transport tubing. Another impinger/mixing chamber was added just before the sampling chamber for all tests. This impinger removed any large resuspended agglomerates, allowing better control over the sampled particle size during the course of the experiments. The chamber also provided a number of additional ports where dilution air could be added and the pressure and humidity measured.

Mass Loading Test Results

The first series of tests duplicated the aerosol generation and filter collection parameters for two mass loading tests in order to show that the experiments were reproducible and to quantify the amount of error inherent in the experiments. Measurements were made by collecting aerosols on a 47mm filter until a desired pressure drop was observed across the filter. The mass on each filter was determined by an analytic balance and by measuring the conductivity of the solution used to wash the filter. Measurements were typically taken at pressure differences of 500,1000,1500 and 2000 Pascal (2,4,6, and 8 inches of water) above the initial pressure drop through the clean filter. Supplementary measurements were obtained with a Tapered Element Oscillating Microbalance (TEOM), a real time mass collection device. Problems with the reliability and reproducibility of the TEOM in the larger size ranges, limited its usefulness in these experiments. However, as Figure 6 indicates the TEOM was able to confirm the essentially linear behavior of the mass loading as a function of pressure drop. This justifies fitting the 47mm filter data with a linear least squares fitting routine. Four sets of 47mm filter data were collected for the TSI generator using a 10% NaCl solution concentration. These tests are overlayed with the Novick and Higgins data set[13] and shown in

Figure 7. The particle sizes measured for these four tests are shown 20% larger than those measured for the Novick and Higgins test for the same generation and sampling conditions.. This difference is most probably due to the improved transport properties of the redesigned experimental system. Note that the reproducibility in particle size, determined by the average between cascade impactor measurements just before and after each mass loading test, between the four tests is excellent. The spread in the data for this particular generator, solution concentration and flow rate (TSI, 10% NaCl and 2.45 cm/s) is approximately ± 7% from the average of all of the data points.

Figure 8 presents the data from four sets of 47mm filter tests compared with the Novick and Higgins results for the Retec generator with a 10% NaCl solution concentration at a filter media velocity of 2.45 cm/s. Again the particle size distribution transported by the new system is larger than that measured in the Novick and Higgins test. The spread in the data for this set of conditions is approximately ± 12%. Both of these measures of the scatter in experimental data is consistent with the error expected from an analysis of the uncertainty in each of the measuring devices. Some of the error may be attributed to particle size differences between tests.

Figures 6 through 12 present examples of the data obtained for each test using a different particle size distribution. In all, nine different particle size distributions were measured. As stated earlier, the TEOM confirms the essentially linear behavior of the mass loading as a function of pressure drop. Therefore, each data set was fit with a linear function using the standard least squares routine contained in the Cricket Graph software. The particle size tests were limited at the low end by the time required to obtain a pressure drop of 2000 Pascal (8 inches of water) across the filter. For the smallest size tested, MMD = 0.66 μm, a continuous collection time of 14 hours was required. The large particle size limit was determined by the transport efficiency through the experimental system. Increasing the solution concentration beyond 10% with the Retec generator resulted in no increase in particle size distribution.

Clearly, Figures 6 through 12 show that varying amounts of aerosol material van be collected on the filter for a given increase in pressure difference. As discussed previously, it is common practice to define the specific resistance of a filter as the increase in pressure difference for a given amount of mass per unit filter area at a given velocity, so that comparisons between filters can be made. In this work, the measured specific resistance ranges from 3.9×10^5 s^{-1} to 1.4×10^6 s^{-1} for particle mass median diameters ranging from 1.7 μm to 0.7 μm. Comparisons between the specific resistance for particles in this size range, can be made with other researchers.

Rudnick and First[12] tested Arizona road dust on four woven fabric filters and measured specific resistances between 5.5×10^5 s^{-1} and 1.0×10^6 s^{-1}. Apparently, the particle size distribution was only measured once from a portion of the dust batch and not for each experiment. The particle size is given as an area median of 0.5 μm with an approximate standard deviation of 1.73. This would mean that the nominal mass median particle diameter for the Arizona road dust experiments was 0.68 μm, which is within the range of particle size tested in this work using NaCl. Note that the measured specific resistance of the road dust is also within the range measured for the NaCl.

Durham and Harrington[14] also measured the specific resistance for three types of glass fiber

filters using fly ash. Specific resistances ranging between 4.3 X 10^4 s^{-1} to 7 X 10^4 s^{-1} at a relative humidity of 30%. The particle size in these experiments was also only measured once from the fly ash batch by dispersing a small quantity in a liquid and using a Coulter counter. The resulting measured mass mean diameter was 4 μm. Optical measurements of the particle size were made for every test, but the authors only reported that the range of particle size remained between 1 μm and 25 μm throughout the tests.

Specific resistances can also be calculated from the data given by McCormack[15]. These mass loading tests were conducted with a variety of HEPA filters, of which the type designated 1 appears to be the same as the Savannah HEPA filter. The test aerosol was generated by burning sodium in air with steam added in some tests, to increase the relative humidity from aerosol 40% to near 60%. The calculated values of the specific resistance ranged from 8.7 x 10^4 s^{-1} to 6.4 x 10^5 s^{-1}. In general, the larger values occurred at higher humidities and lower flowrates. The particle size measured in these tests ranged from 1.4 μm to 6.8 μm, averaging 3 μm for the mass median aerodynamic diameter. However, the particle size was not measured for every test. Clearly, the larger fly ash and sodium hydroxide particles have lower values for the specific resistance compared to the smaller NaCl or Arizona road dust.

Examination of Figures 9 through 12 show a similar relationship between the slope of the line which is the specific resistance, K_2, and the mass median particle diameter representative of the aerosol distribution. Figure 13 presents a graphic presentation of all the mass loading data from tests denoting the relationship between the mass loading per unit area per unit pressure difference (i.e., the inverse slope) and the mass median particle diameter. Clearly, the specific resistance decreases as the particle diameter is increased.

In order to compare experimental results with theoretical predictions, thickness measurements were taken of the particle cake for a number of tests. The porosity of the cake can be calculated from the thickness and cross sectional area of the cake and knowledge of the density of the solid particles.

For all data, where thickness was measured, the porosity averaged 0.7 with a standard deviation of almost 50%. The calculated resistance factor based on the the porosity of each test, R, however, has a standard deviation on the order of 200%, from an average of 21, clearing indicating that either a better method for determining R is required or that R has a functional dependence on some experimental parameter. On the other hand, using Equation (8) for the same data set, the average value of R_{exp} is 6.8 with a standard deviation of 35%.

Another method of determining R, that is instructive, is to take the slope, K_2 of each of the pressure drop vs. mass loading curves. This slope is essentially an average of the $(\Delta P-\Delta P_o)/(M/A)$ measurements for that particular velocity and particle size. Dividing the slope by the velocity and plotting the results as a function of the inverse of the particle diameter squared, is a convenient method of combining all of the data on one graph. The slope of this line should simply equal R times some constants as indicated from Equation (8). However, Figure 14 shows that the data clearly has a y-intercept, indicating that R is also a function of the particle size. The slope from Figure 4 defines R

to be

$$R = 3.06 + 7.56 \times 10^7 \rho_p \, CD^2 \qquad (9)$$

The density and particle size are in cgs units. This method of determining R has a standard deviation of only 20% which is much closer to that expected from the analysis of errors in the experiment.

Conclusions

The HEPA filter media is at least 99.99886% efficient for all dry particles sizes traveling with a gas whose velocity is 0.89 cm/s. The media is at least 99.9727% efficient for particle and gas velocity at 2.98 cm/s. These measured efficiencies meet or exceed current specifications. Efficiency spectra were determined for both flow rates allowing the release to the environment to be calculated for a given particle size distribution.

The resistance factor, R, was shown to be dependent on the mass median particle diameter for polydisperse aerosol distributions. This contradicts the assumption that the resistance factor, itself, is independent of particle size. However, as particle diameter decreases, the resistance factor does indeed become a constant according to Equation (9).

Combining Equation (9) and Equation (8) allows the mass loading per unit area to be predicted for a desired increase in pressure differences across the filter, a given velocity and known or estimated mass median particle diameter.

$$M/A = (\Delta P - \Delta P_o) \, C\rho_p D^2 / 18 \, V \mu \, (3.06 + 7.56 \times 10^7 \rho_p \, CD^2) \qquad (10)$$

Equation (10) also uses cgs units for all terms. This equation accounts for variations in particle diameter, particle density, gas viscosity and gas velocity. Therefore, it can be generalized to a wide variety of filtration scenarios within certain limitations.

One limitation is that the model described by Equation (10) is only good for dry, solid particles. Wet soluble particles appear to produce an exponential increase in pressure drop as the aerosol mass is increased in the filter. This effect was also seen by McCormack[15] using sodium hydroxide-aerosols. It is probable that insoluble particles with a liquid coating also exhibit non-linear behavior. However, Durham and Harrington[15] Ariman and Helfritch[16] showed that for some combination of aerosol and filter materials, the specific resistance of a filter cake decreased as the relative humidity was increased from 20% to 60% and from 20% to 80% respectively. This effect has not been quantified or incorporated into the model.

Another limitation is the extension of Equation (10) to other materials and shapes. Based on the agreement between Rudnick's data for Arizona road dust and this work with NaCl, in measuring the

porosity of the particle cake, Equation (10) should be applicable to a wide variety of materials that are relatively non-sticky. In addition, based on the observation by Kozeny and Carmen of a 4% difference between spherical and irregularly shaped particles, Equation (10) should be applicable to most particles with aspect ratios near unity. Flakes and needles would probably have significantly different porosities and hence different values for the resistance factor. Finally, there may be limitations on the applicable particle size range of equation (10). Very small particles with high adhesive coefficients may cause variations in the cake porosity in a manner similar to the 'sticky' particles mentioned earlier. Also, particles with a size corresponding to the minimum efficiency of the filter material may cause an initial non-linear increase in pressure differential as a function of mass loading.

In general, the highly efficient collection capabilities of this filter media, cause a particle cake to be formed very rapidly on the surface of the filter. Measurements indicate that this cake forms in the first few minutes of aerosol collection. This phenomena allows the use of Equation (10) for predicting mass loadings on the Savannah River HEPA filter material.

Acknowledgement

The authors would like to acknowledge the U.S. Department of Energy, Nuclear Energy Group, for supporting this work under Contract No. W-31-109-eng-38.

References

1. Petry, S.F., et al, L-Area Ventilation Tests - 1984, SRL Report DPST-85-336, March 1985.

2. Savannah River Plant Specifications DPSOP 40-2, Spec.4.

3. Tinnes, S.P., and Petry, S.F., System Analysis Airborne Activity Confinement System of the Savannah River Production Reactors, SRL Report DPSTSY-100-10, March 1986.

4. Durant, W.S., et al, Activity Confinement System of the SRP Reactors, SRL Report DP-1071, August 1966.

5. Lee, K.W., and Liu, B.Y.H., "Experimental Study of Aerosol Filtration by Fibrous Filters," Aerosol Science and Technology 1:35-46 (1982).

6. Liu , B.Y.U., Pui, D.Y.H., and Rubow,K.L., "Characteristic of Air Sampling Filter Media," Aerosols in the Mining and Industrial Work Environment, Marple, V.A., and Liu, B.Y.H., Editors, Ann Arbor, Michigan, 1983.

7. Berglund, R.N., and Liu, B.Y.H., "Generation of Monodisperse Aerosol Standards," Environ. Sci. Tech. 7:147-152, (1973).

8. Knutson, E.O., and Whitby, K.T., "Accurate Measurement of Aerosol Electric Mobility Moments," J. Aerosol Sci. 6:453-460, (1975).

9. Wark, K., and Warner, C.F., Air Pollution, Harper and Row, New York (1981).

10. Leith, D., and Allen, R.W.K., in Progress in Filtration and Separation 4 (R.J. Wakeman Ed.) Elsevier, New York (1986).

11. Wakeman, R.J., Progress in Filtration and Separation 4 (R.J. Wakeman Ed.) Elsevier, New York (1986).

12. Rudnick, S.N., and First, M.W., "Specific Resistance (K_2) of Filter Dust Cakes: Comparison of Theory and Experiments," in the Third Symposium on Fabric Filters for Particulate Collection EPA-600/7-789-087 (June 1978).

13. Novick J.D., and Higgins, P.J., Westinghouse Savannah River Report WSRC-RP-89-793 (1989).

14. Durham, J.F., and Harrington, R.E., "Influence of Relative Humidity on Filtration Resistance and Efficiency of Fabric Dust Filters," Filtration and Separation, July/August (1971).

15. McCormack, J.D., Hilliard, R.K., and Barreca, J.R., "Loading Capacity of Various Filters for Sodium Oxide/Hydroxide Aerosols," 15th DOE Nuclear Air Cleaning Conference CONF 780819 (1979).

16. Ariman, T., and Helfritch, D.J., "How Relative Humidity Cuts Pressure Drop in Fabric Filters," Filtration and Separation 14: 127-130 (1977),.

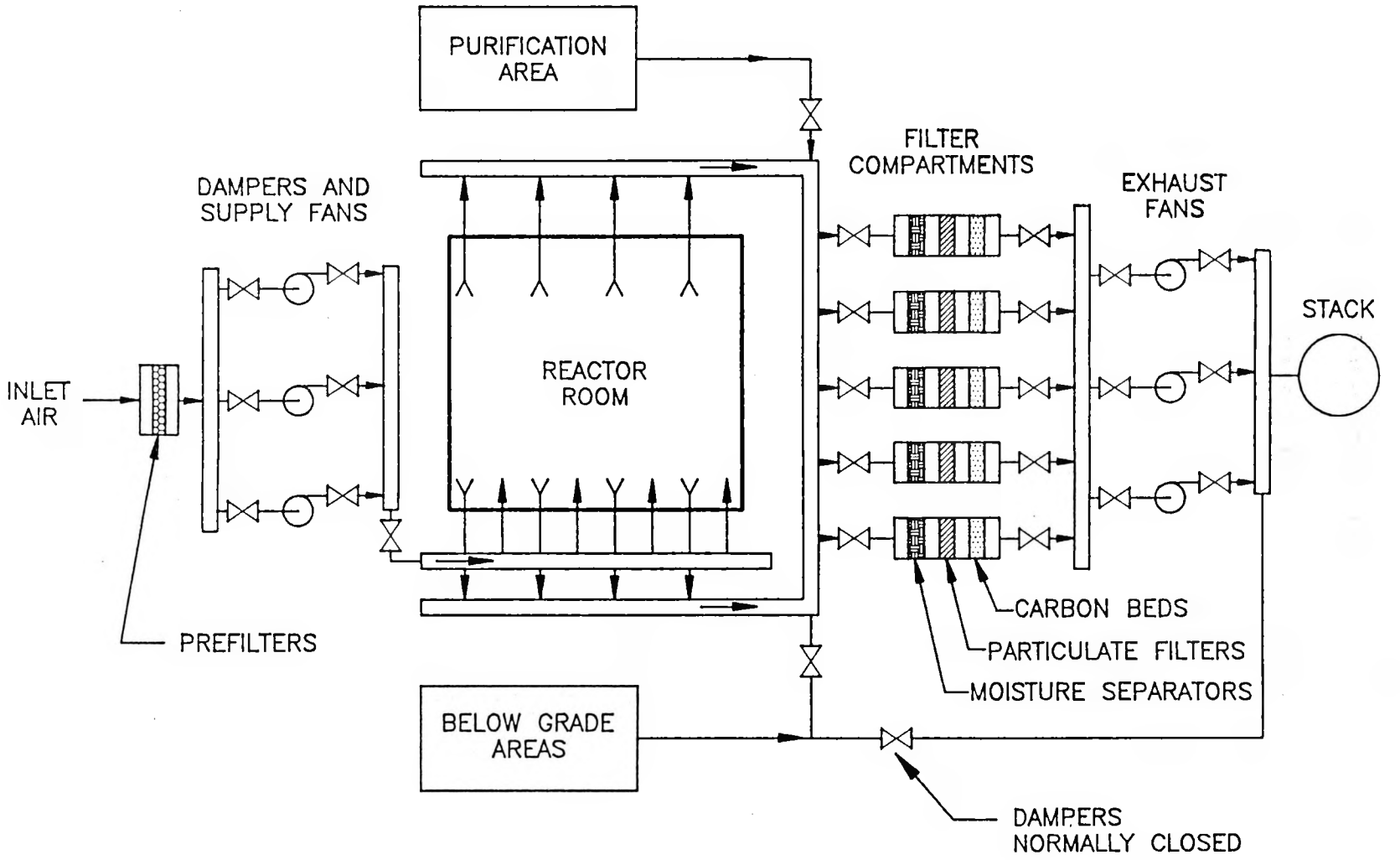

Figure 1. Schematic of the Airborne Activity Confinement System (AACS)

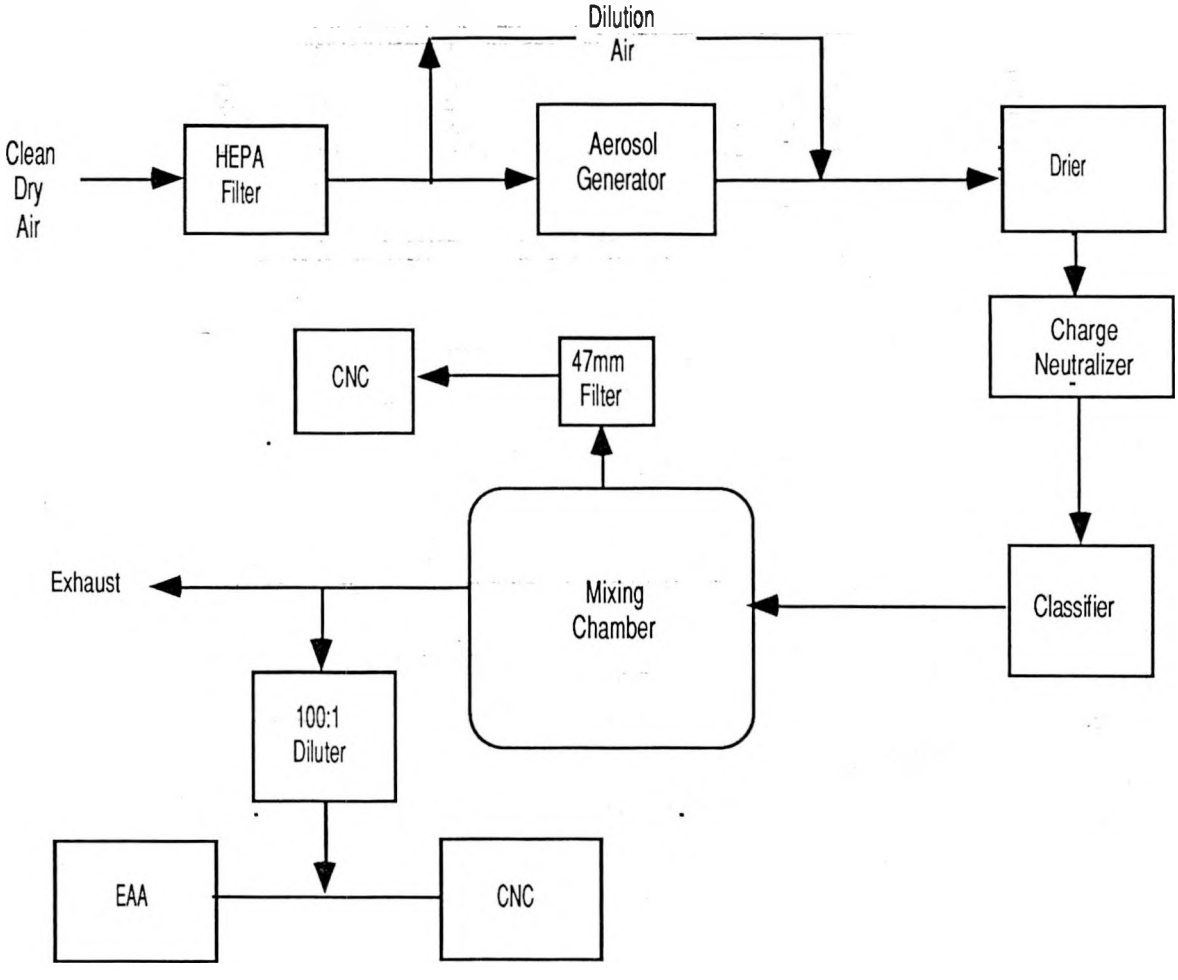

Figure 2. Experimental Configuration for Efficiency Tests

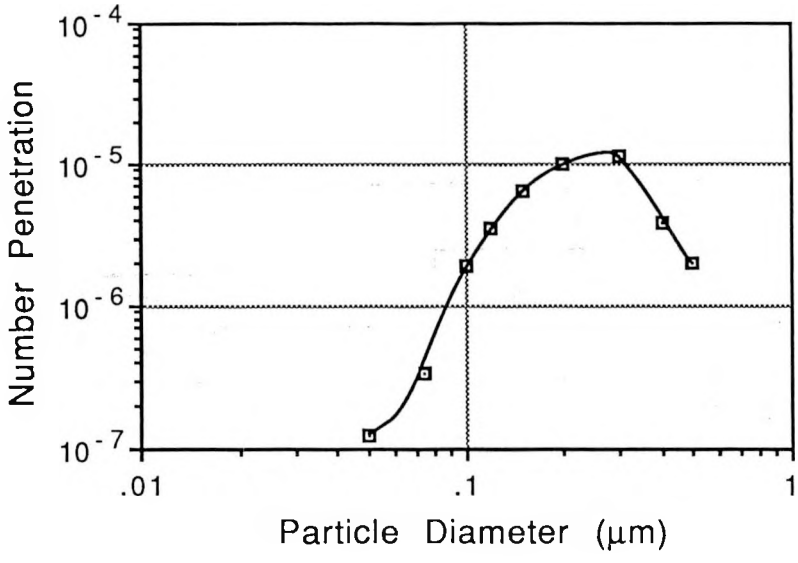

Figure 3a. Number Penetration Versus Particle Diameter for Monodisperse NaCl Aerosols Using an Electrostatic Classifier, Filtration Velocity = 0.89 cm/s

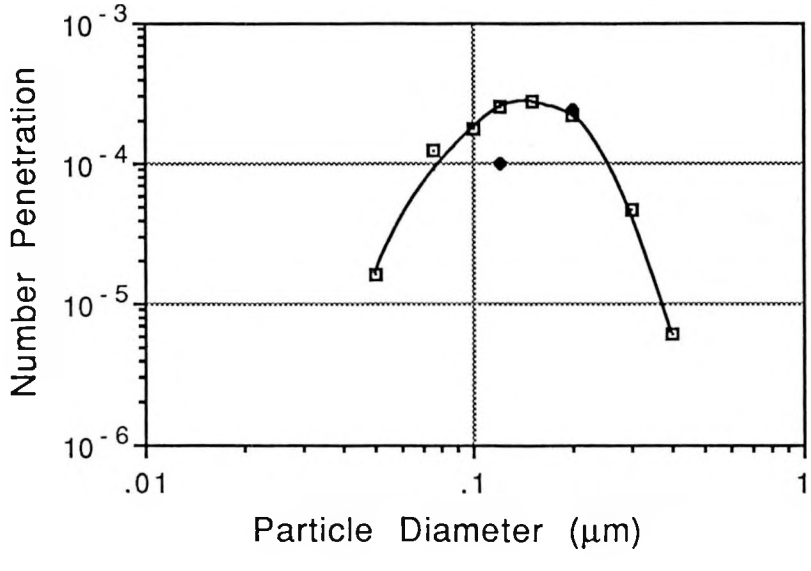

Figure 3b. Number Penetration Versus Particle Diameter for Monodisperse NaCl Aerosol Using an Electrostatic Classifier, Filtration Velocity = 2.98 cm/s

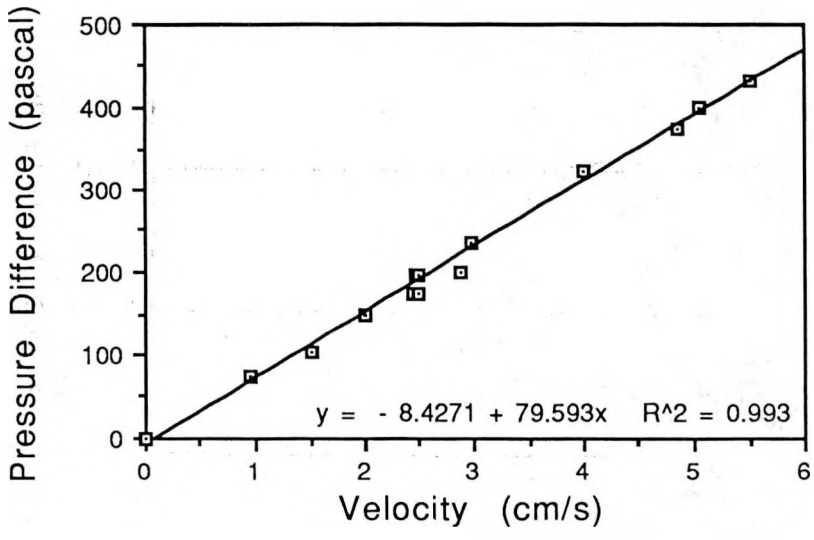

Figure 4. Filtration Velocity Versus Pressure Difference for Clean 47mm HEPA Filter

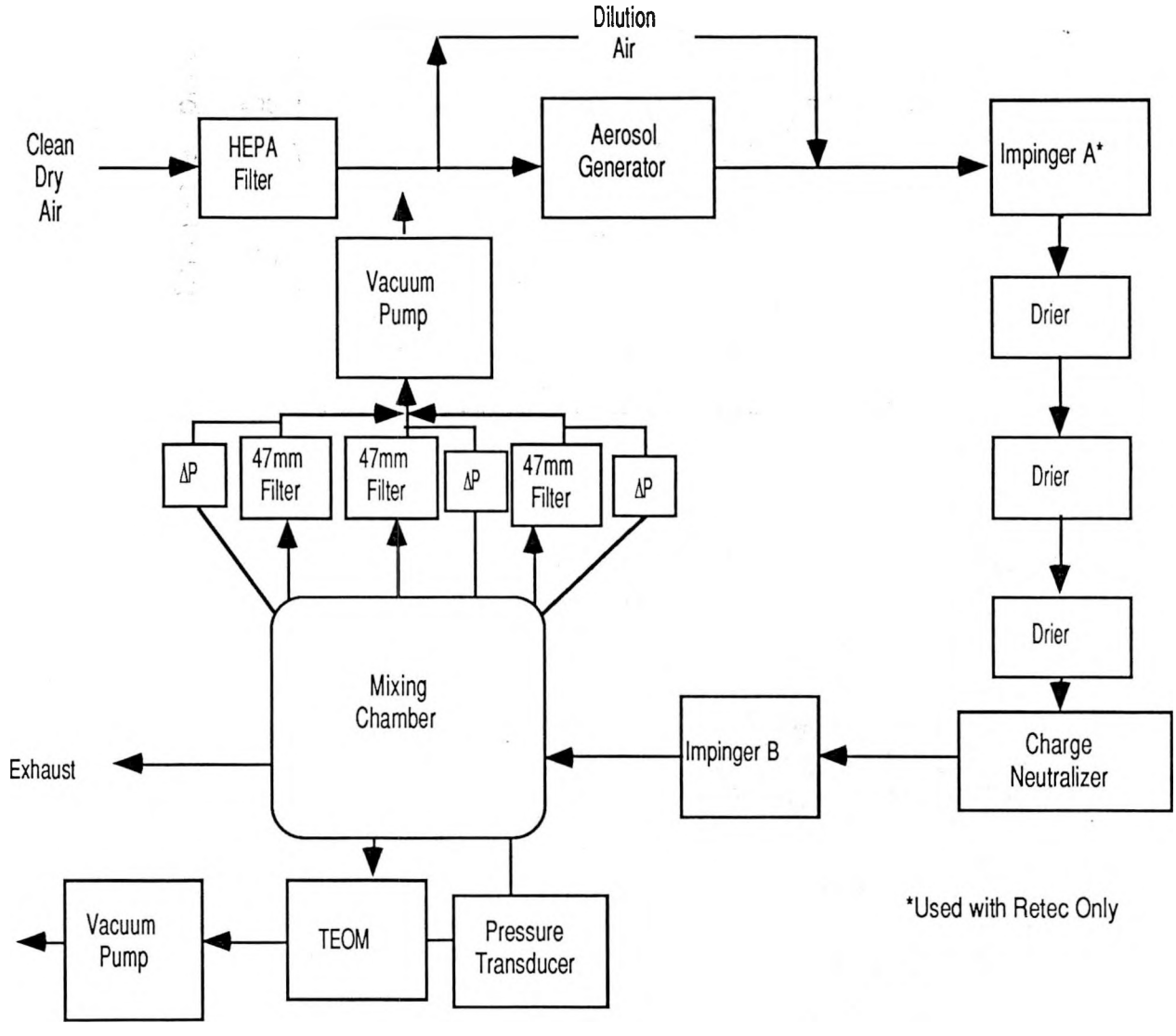

Figure 5. Experimental Configuration for Pressure Difference Versus Mass Loading Tests

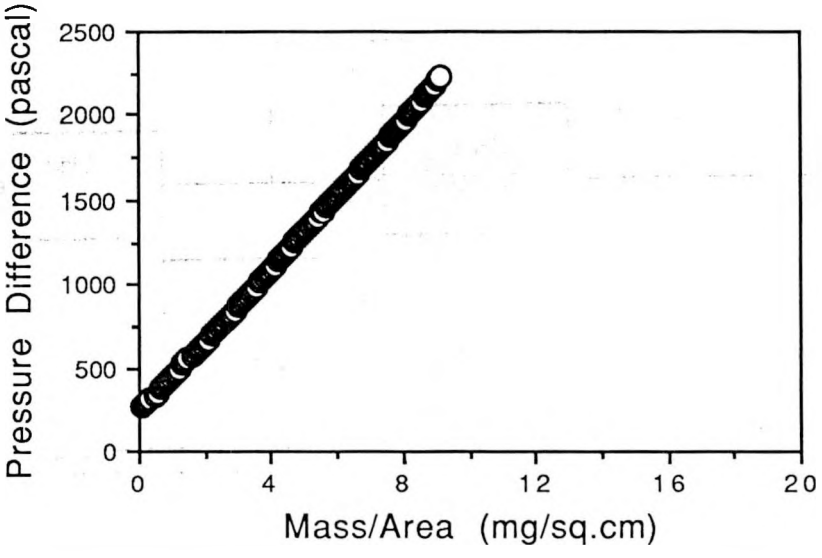

Figure 6. Example of Linear Increase of Mass Loading with Pressure Drop Using the TEOM

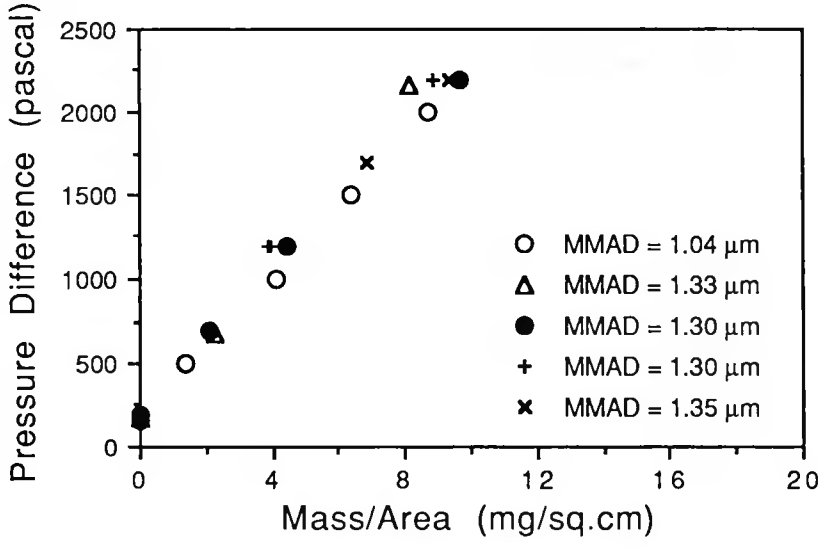

Figure 7. Tests Comparing the Pressure Difference Versus Mass Loading Using the TSI Atomizer with a 10% Solution (Velocity = 2.45 cm/s)

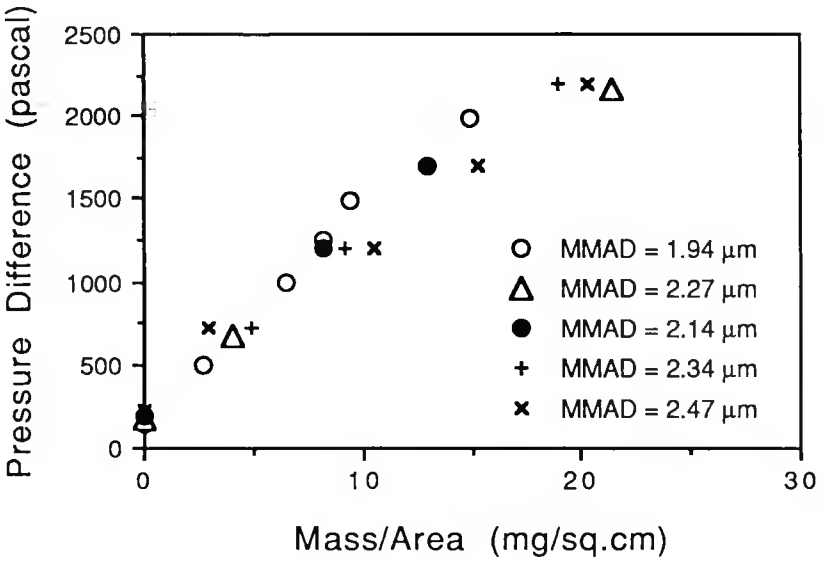

Figure 8. Tests Comparing the Pressure Difference Versus Mass Loading Using the Retec Nebulizer with 10% Solution (Velocity = 2.45 cm/s)

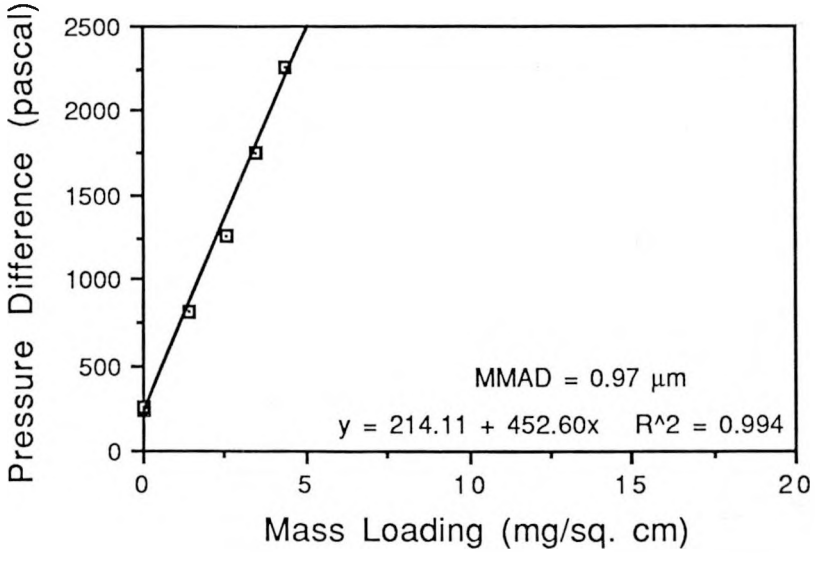

Figure 9. Pressure Difference Versus Mass Loading for a Particle Size Distribution with a MMD = 0.66 µm (TSI Atomizer, 2% Solution, V = 3 cm/s)

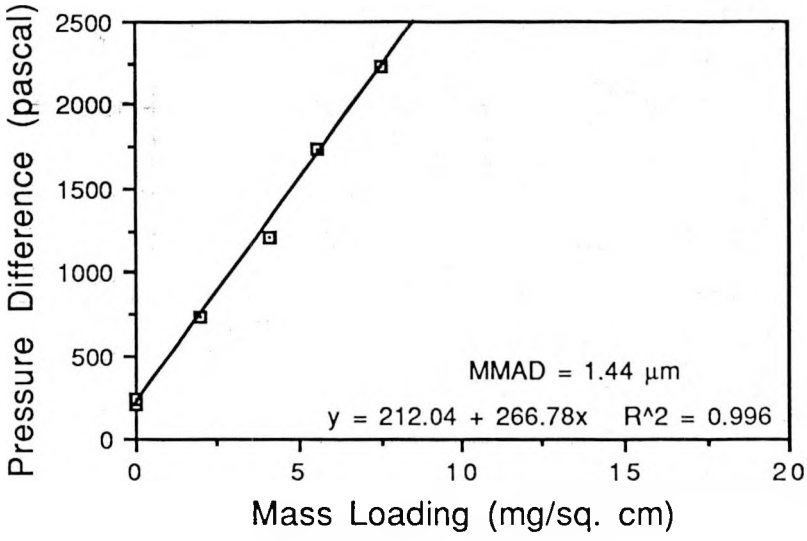

Figure 10. Pressure Difference Versus Mass Loading for a Particle Size Distribution with a MMD = 0.99 µm (TSI Atomizer, 15% Solution, V = 3 cm/s)

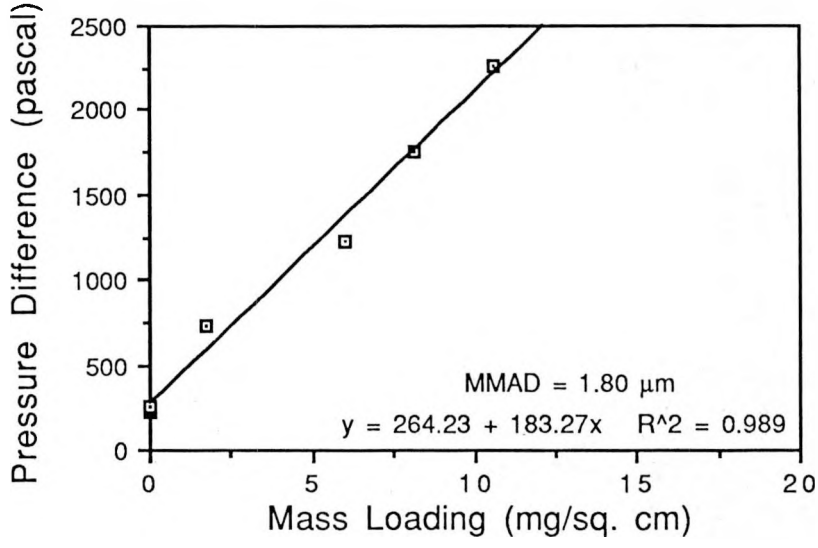

Figure 11. Pressure Difference Versus Mass Loading for a Particle Size Distribution with a MMD = 1.23 µm (Retec Generator, 10% Solution, V = 3 cm/s)

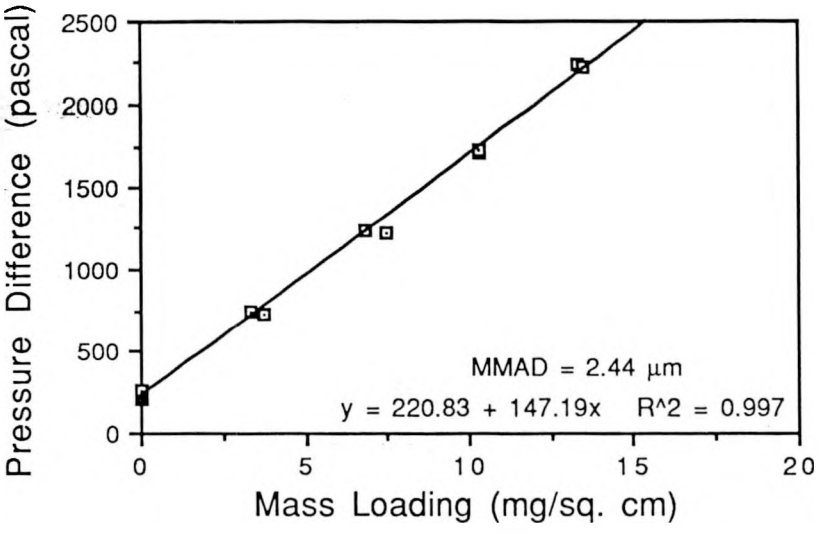

Figure 12. Pressure Difference Versus Mass Loading for a Particle Size distribution with a MMD = 1.69 µm (Retec Generator, 10% Solution and 4% Solution, V = 3 cm/s)

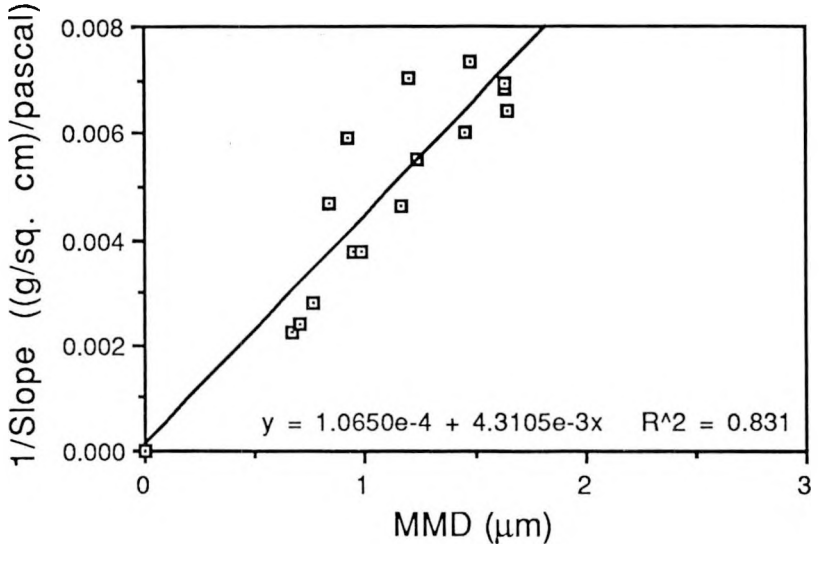

Figure 13. Mass Loading Per Unit Area Per Unit Pressure Difference Versus Particle Size for All Data with V = 3 cm/s

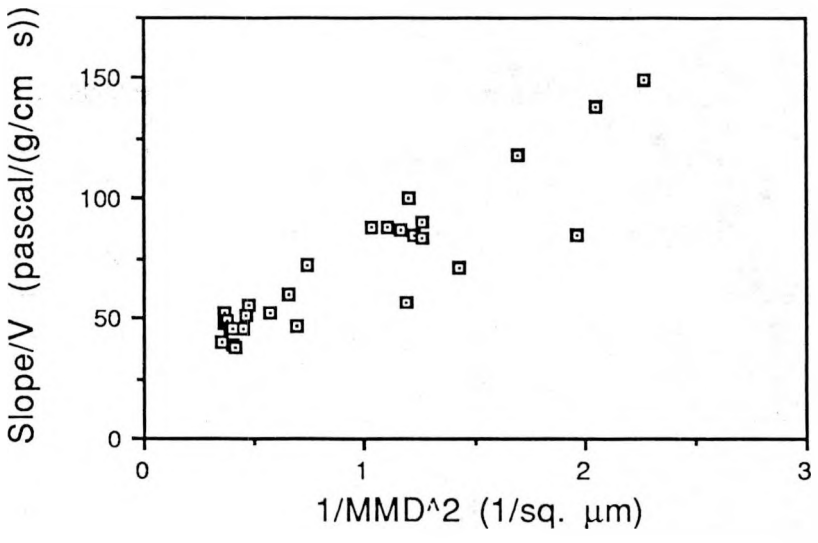

Figure 14. Slope/V as Determined by the DP/V(M/A) From the Mass Loading Versus Dp Curves, as a Function of Particle Size